Journal of Ovonic Research Vol. 16, No. 5, September - October 2020, p. 253 - 259

STUDY OF THE MORPHOLOGICAL TRANSFORMATION OF COPPER IODIDE NANOSTRUCTURES PREPARED BY SUGAR BEET MEDIATED ROUTE

R. JAVAID, H. ANWAR*, Y. JAMIL, B. ABBAS, M. IQBAL, S. AHMED, A. ISLAM, F. BATOOL, M. KHALID, U. ELAHI, S. RIAZ, K. HAYAT
Department of Physics, University of Agriculture, Faisalabad-38040 Pakistan

Copper Iodide (CuI) is a p-type semiconductor and is significant owing to vital applications especially in semiconductor electronic devices. Recently, in Perovskite solar cells CuI as hole transport material (HTM) reveals a promising efficiency over 21.0 % which is highest among the reported efficiency at room temperature. In this research, CuI nanostructures were prepared by green method using sugar beet juice with different concentrations (5 ml, 10 ml, 15 ml and 20 ml). In this method, sugar beet juice was used as reducing and capping agent thus controls particle size. The as prepared samples were investigated by X-ray diffraction (XRD), scanning electron microscopy (SEM), Energy dispersive X-ray spectroscopy (EDX) and UV-vis spectroscopy. The XRD analysis confirmed the pure cubic structure of copper iodide nanostructures and average crystallite size was found to decrease with an increase in the concentration of beet juice in the range of 43 nm to 31 nm. SEM showed the morphological transformation. SEM images showed that CuI nanostructures were triangular like shape at lower concentration but at higher concentrations nanosheets like shape were observed. EDX confirmed the presence of iodide and copper with proper composition. UV-visible spectroscopy results revealed the variation of band gap energy with increasing concentration of beet juice. Morphological transformation can be critical in optoelectronic devices regarding charge transfer at different interfaces.

(Received April 4, 2020; Accepted September 3, 2020)

Keywords: Copper iodide, Sugar beet juice, Morphological transformation

1. Introduction

Wide band gap semiconductors having p-type electrical conductivity has extensive research attention because of their vital applications in semiconducting electrical devices. These semiconductors mostly used in photovoltaic technology, i.e., it served as hole transport material (HTM) in perovskite solar cells. Great potentials for the integration with the perovskite design of an optoelectronic device have been verified by copper iodide. It signifies a cost-effective inorganic material [1]. Copper iodide (CuI) is termed marshite as a mineral when Charles W. Marsh, who 1st noted this mineral at Broken Hill, Australia [2]. Copper iodide also known as cuprous iodide. It is a wide band gap p-type semiconductor (Eg 3.1 eV), which has vital uses in countless fields [3]. Cuprous Iodide belongs to the I–VII semiconductors with Zinc-blende structure [4]. It is a direct semiconductor with zinc blende structure below 643 K (γ-CuI), a wurtzite structure between 643-673 K (β-CuI) and a rock salt structure above 673 K (α-CuI) [5]. CuI has fascinated attention due to its unique properties, for example, wide band gap, negative anomalous diamagnetism behavior, large ionicity and spin–orbit splitting [6]. CuI has been effectively applied in scintillators, bi-polar diodes and organic electronics. The advancement in high excellence bipolar diodes reveals the use of copper iodide in transparent electronics [7].

In 1907, Copper iodide also known to be transparent semiconductor due to high efficiency. CuI has several benefits, such as this material is environment friendly, it is non-toxic and naturally abundant. of advantages. It is an environment-friendly material composed of nontoxic and

* Corresponding author: hafeez.anwar@gmail.com

naturally abundant elements [8]. Cuprous iodide is water insoluble material. It can easily dissolvable in acetonitrile (CH_3CN) at room temperature [9]. Research on CuI has been extensively discussed in the literature over the past numerous decades. CuI links to cuprous halide family CuX; it is characterized through the mono-valent copper (I) state which is stabilized by tetrahedral coordination to the bounded four halogen atoms. In the crystal-like state, under ambient environments, the solid CuI has a zinc-blend structure with $F\bar{4}3m$ space group. On heating, its FCC (face-centered cubic) lattice endure a series of two-phase transformations, γ-CuI → β-CuI → α-CuI, characterized through transition temperatures 369 ºC and 407 ºC, respectively. Both these polymorphs have diverse crystal structures: β-CuI crystallizes in the hexagonal wurtzite structure (P63mc), while α-CuI returns to the cubic rock salt structure ($Fm\bar{3}m$) [1].

Literature survey shows synthesis of copper iodide via numerous methods, such as using kidney bean [10], pulse laser deposition technique [11], cycle evaporation method [12], sonication [13], co-precipitation [14,15], microwave-assisted method [16], using ampicillin [17], micro-emulsion, [18], solvo-thermal methods [19], hydrothermal methods [3], by using pomegranate juice [20], glucose [21], watermelon, cheery, carrot juice [22]. Although Copper (I) iodide nanoparticles synthesized by chemical method [23] showed good dispersion in the suspension, it resulted in formation of an impure product. Therefore, there was a need for a method that employs less chemicals and gives high purity product. Synthesis of copper iodide nanoparticles using green chemistry is environment friendly, non-toxic and less use of chemicals. In synthesis of nanoparticles the extracts from plants may act as both capping and reducing agents. Generally, fruits or plants extract control particle growth by acting as stabilizers, capping and reducing agents [10].

Anthocyanin molecules present in sugar beet act as capping and reducing agent. Total anthocyanin of the sugar beet molasses extract were 31.81 mg/100g [24]. Anthocyanin is colorful water-dissolvable pigment belonging to phenolic group. The pigments are in glycosylated forms. In vegetables and fruits this anthocyanin is responsible for the colors such as purple, blue and red. Grapes, Berries, currants and some fruits have high content of anthocyanin. [25].

This present study aims to study the morphological transformation of synthesis of CuI nano structures via sugar beet juice that is rich in anthocyanin content and by using simple co-precipitation method. In this work, CuI nanostructures were synthesized with various concentrations of sugar beet juice (5 ml, 10 ml, 15 ml and 20 ml) and without juice. The structural properties of the synthesized CuI NPs were characterized by XRD. The absorption spectrum of these nanostructures was obtained by UV-vis spectroscopy. SEM was used for investigating about morphology and shape of these nanostructures. EDX was used to confirm purity of these nanostructures.

2. Experimental

Copper sulphate and potassium iodide were purchased from Merck Company. All chemicals were used without any further purification. In a typical synthesis potassium iodide solution (0.12 M) was added drop wise into the $CuSO_4$ solution (0.12 M). This mixture was stirred for 30 mins at room temperature. After completion of this reaction, the obtained precipitates then filtered and washed by using filtered water and dried in natural air and labeled as A. We take this sample A as a reference. In next samples we used sugar beet juice (5 ml, 10 ml, 15 ml, 20 ml) with Copper sulphate and potassium iodide were used without further purification. In a typical synthesis, 10 ml sugar beet juice was added into copper sulphate solution (0.12 M) under magnetic stirring, and then potassium iodide solution (0.12 M) was added dropwise into the above solution. The mixture was stirred for 30 mins at room temperature. When the reaction was completed, the resultant precipitate was filtered and washed with distilled water and finally dried in air naturally and labeled as B, C, D and E.

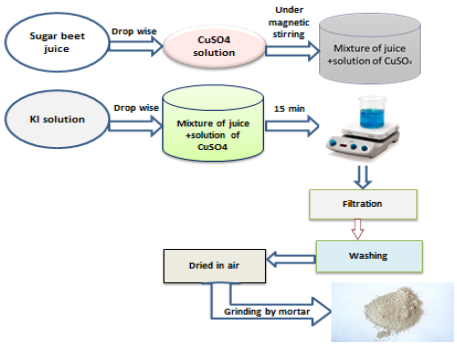

Fig. 1. Synthesis of CuI nanostructures.

2.1. Characterization techniques

The powder X-ray diffraction was performed through XRD system Model PANalytical with Nickel filter CuK_{α} (λ = 1.50405 Å) radiation. The particle size was calculated from broadening of line using Scherer's formula. The scanning electron microscope (SEM) studies were performed using SEM Model (JEOL- JSM 5910) to study the morphology of the prepared nanoparticles. The absorption spectra of samples were recorded with UV-Vis spectrophotometer PG (Model T-80).

The average particle size (D) was estimated by Scherrer formula given as

$$D = \frac{k\,\lambda}{\beta cos\theta} \tag{1}$$

where k is the Scherrer's constant and also known as shape constant having value 0.9 in our case, λ is wavelength of x-rays, β is full width at half maximum (FWHM) and θ is the Bragg angle.

By using the following equation, lattice parameters 'a', b and 'c' of cubic CuI were calculated.

$$\frac{1}{d^2} = \frac{h^2 + k^2 + l^2}{a^2} \tag{2}$$

For cubic structure, the volume can be calculated by

$$V = a^3 \tag{3}$$

and X-ray density can be calculated by

$$\rho = \frac{nM}{N_A V} \tag{4}$$

M is the molecular mass of CuI which is 190.45 g/ mol, N_A is Avogadro's number and its value is constant (6.02×10^{23} mol^{-1}). n is the number of atoms per unit cell.

3. Results and discussion

3.1. Structural analysis

The XRD pattern of prepared copper iodide nanoparticles at different concentrations samples A, B, C, D and E are shown in Fig. 2. All these reflection peaks can be simply indexed to pure cubic crystal phase of nano-crystalline CuI. Similarly, no extra peaks because of impurities were observed. It is clear that both have cubic structure. All reflection peaks with high intensity verified the high crystallinity of these prepared nanostructures. The sharp and broad peaks (111),

(220) and (311) are located at 2θ values of 25.50º, 29.53º and 50.01º respectively. Other peaks (220), (222), (400), (331) and (420) have positions at 42.27º, 52.41º, 61.27º, 67.39º and 69.42º respectively [22]. The XRD pattern of these CuI nanostructures are exactly matched with JCPDS card for cubic CuI.

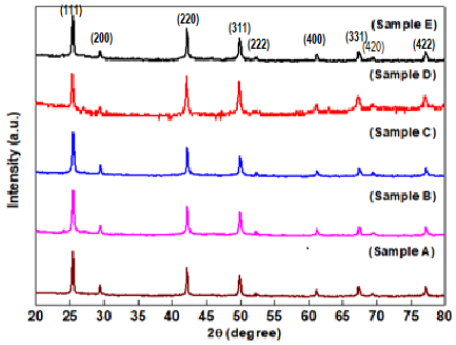

Fig. 2. XRD pattern of prepared pure and CuI at different concentrations.

The calculated average crystallite size for Sample A found to be 46 nm. Average particle size for samples B, C, D and E found to be 43, 32, 31, 38 nm, respectively. It is found that by increasing concentration of juice particle size is getting reduced. This is because of anthocyanin molecules present in juice which acts as a reducing and capping agent and controls the particle size. But in case of sample E, it shows that there starts agglomeration that causes an increase in particle size.

Table 1. Structural parameters of prepared CuI nanostructures extracted from XRD.

Sr. No	Sample	Average Crystallite size (nm)	Lattice Parameters a=b=c nm	Volume $(nm)^3$	Density g/cm^3
1	A (without juice)	46	0.6063	0.2228	5.67
2	B (5 ml)	43	0.6404	0.2627	4.81
3	C (10 ml)	32	0.6049	0.2213	5.71
4	D (15 ml)	31	0.6074	0.2241	5.64
5	E (20 ml)	38	0.6064	0.2229	5.67

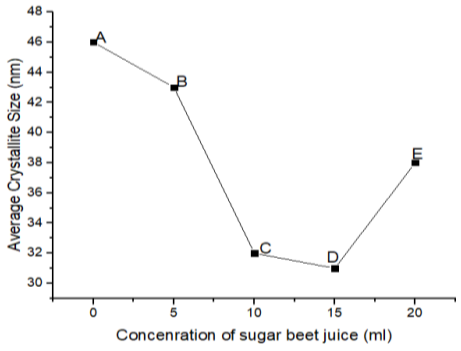

Fig. 3. Variation in average crystallite size with different concentrations of sugar beet juice.

3.2. SEM Analysis

Scanning electron microscopy (SEM) micrographs of samples A, C and E shown in Fig. 4. Fig. 4 (a) showed agglomerated irregular shapes with random sizes for the sample A without sugar beet juice whereas for 10 ml juice sample C triangular-like structure was observed [fig 4 (b)]. For sample E with 20 ml juice, nanosheets were observed [Fig 4 (c)]. These morphological transformations are due to the anthocyanin molecules in sugar beet juice that acted as capping agent and played its role to control size and shape of the nanostructures.

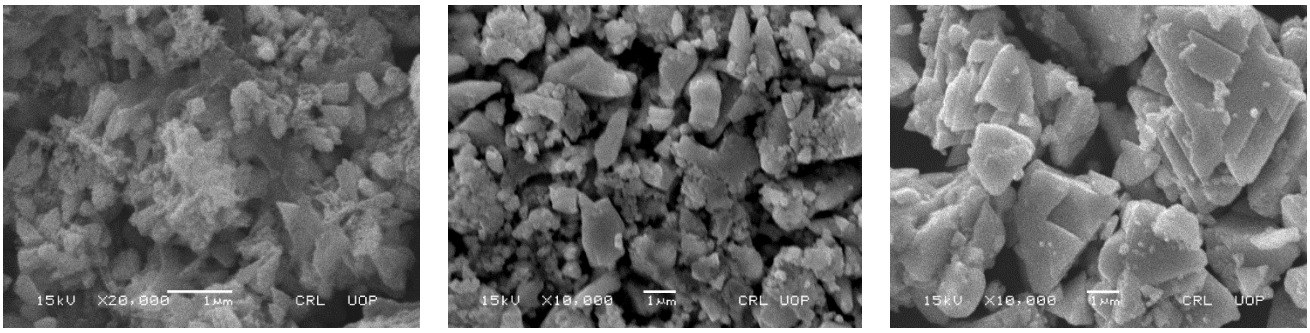

(a) *(b)* *(c)*

Fig. 4. SEM micrographs of CuI nanostructures (a) without sugar beet juice (b) 10 ml juice (c) 20 ml juice

3.3. EDX Analysis

The chemical purity and stoichiometry of Sample C was investigated by the EDX spectrum as shown in Fig. 5. The peaks were initiating from Cu, I, O and C only. An elemental ratio of Cu:I of unity is in good agreement by stoichiometric ratio. Here C tells about the carbon grid that used for deposition of nanoparticles and carbon used in juice. This analysis showed a good agreement with the XRD data.

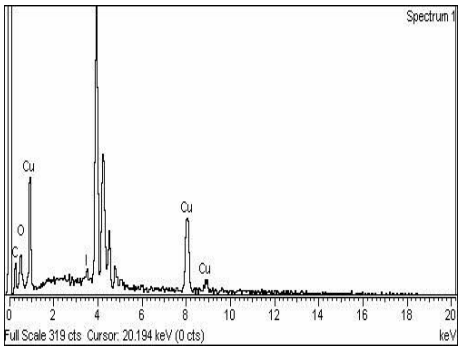

Fig. 5. EDX analysis showing the elemental composition of Sample C.

3.4. UV-Vis Analysis

UV spectroscopy used to characterize the absorbance spectrum of these samples. An absorption onset about 270 nm is perceived for these samples. The band gap was calculated by using absorbance data. The band gap was calculated with the help of Tauc and Davis Mott relation. The equation is as follows

$$(\alpha\, h\, \nu)^n = k\,(h\,\nu - E_g) \tag{5}$$

In this relation n is taken as 2 showed the nature of the transition. The hν indicated the photon energy and k is energy independent co-efficient. E_g denotes the optical band gap. The α is

absorption Co-efficient and was calculated by using Beer lambert law. Figure (6) exhibited the absorption spectrum of CuI nanostructures.

Results revealed that CuI nanostructures have strong absorption. The wavelength corresponding to the absorption ranges between 250-600 nm. The band gap calculated by Tauc plot method was 4.90 eV, 4.87 eV, 4.83 eV, 4.79 eV for sample B, C, D and E respectively. The band gap was decreased with slightly increase in the concentration of the sugar beet juice as shown in Fig. 6. The absorption of the incident radiation depends upon the shape and size of the nanoparticles. The band gaps of copper iodide nanostructures were obtained from plot between hν vs $(\alpha h\nu)^2$ are shown in inset of Fig. 6. The results revealed that the band gap decreased with increased in sugar beet juice in the copper iodide nanoparticles which showed red shifting. The value of band gap is more than previously reported literature (4.71 eV) and this higher value of band gap might be due to a quantum confinement effect [26].

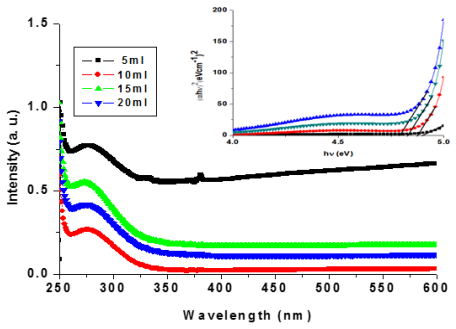

Fig. 6. UV-vis spectrum of different concentrations sample B, C, D, E. Inset: plot $(\alpha h\nu)^2$ vs hν.

4. Conclusion

In summary, CuI nanostructures with different morphologies have been successfully prepared via green, cost effective, fast and effective method at room temperature. The XRD data showed that all peaks matched well with those of the pure cubic phase, and the EDS analysis confirmed the formation of a 100% pure CuI compound. The SEM images showed that size and morphology of these nanostructures can be effectively controlled by varying the concentration of sugar beet juice. Morphological transformation from irregular pattern to nanosheets via anthocyannin molecules present in sugar beet juice. Sugar beet juice act as reducing and capping agent to control average crystallite size. By UV- vis spectrum the maximum absorption peaks were detected and calculated band gap via Tauc Plot method. In addition, the optical absorption of colloidal solution shows a strong blue shift as compared to bulk absorption.. This green synthesis has a great efficiencey for the advancement and application of the perovskite solar cells (PSC) for industrial purposes.

Acknowledgments

Authors acknowledge the funding of Higher education commission Pakistan under project No: NRPU/8545.

References

[1] A. Pishtshev, S. Z. Karazhanov, The Journal of Chemical Physics **1**, 37 (2017).
[2] M. Grundmann, F. Schein, M. Lorenz, T. Bontgen, J. Lenzner, H. Wenckstern, Physica Status Solidi (A) Applications and Materials Science **1671**, 1703 (2013).
[3] B. Abdollahi Nejand, V. Ahmadi, H. R. Shahverdi, Materials Letters **138**, 140 (2014).

[4] P. V. C. Luhanga, C. Muiva, S. H. Coetzee, K. Maabong, L. Tiedt , P. Monowe J. Optoelectron. Adv. M. **837**, 841 (2016).
[5] T. Baran, S. Wojtyła, A. Dibenedetto, M. Aresta, ChemSusChem **1**, 7 (2016).
[6] P. Gao M. Gu, X. Liu, B. Liu, Y. Zheng, E, Shi, J. Shi, G. Zhang, Journal of Alloys and Compounds **170**, 173 (2014).
[7] C. Yang, M. Kneiß, F. L. Schein, M. Lorenz, M. Grundmann, Scientific Reports **1**, 8 (2016).
[8] S. Jaschik, M. R. G. Marques, M. Seifert, C. Rödl, S. Botti, M. A. L. Marques, Chemistry of Materials **7877**, 7822 (2019).
[9] J. Zhou, D. Sun, L. Wang, L. Guo, W. Chen, F. Yu, Y. Wang, Y. Yang, Journal of Membrane Science **142**, 149 (2019).
[10] A. Vijayakumar, R. Rajagopal, International Journal of Scientific & Engineering Research **602**, 609 (2016).
[11] A. Tanji, I. Akai, K. Kojima, T. Karasawa, T. Komatsu, Journal of Luminescence **516**, 518 (2000).
[12] J. Pan, S. Yang, Y. Li, L. Han, X. Li, Y. Cui, Crystal Growth and Design **3825**, 3827 (2009).
[13] A. Ziarati, J. Safaei-ghomi, S. Rohani, Ultrasonics Sonochemistry **1069**, 1075 (2013).
[14] Y. Xu, S. Yang, G. Zhang, Y. Sun, D. Gao, and Y. Sun, Materials Letters **1699**, 1702 (2011).
[15] G. Mustafa, M. U. Islam, H. Anwar, M. Asif, M. I. Arshad, N. Sabar, M. R. Ahmad, G. Murtaza, M. A. Bashart, A. Ali, M. R. Saleem, H. Akhtar, Journal of Ovonic Research **261**, 267 (2018).
[16] J. Li, H. Zhao, H. Jia, L. Zhang, Y. Gao , Z. Zheng, Chemistry Letters **68**, 69 (2011).
[17] Y. Jiang, S. Gao, Z. Li, X. Jia, and Y. Chen, Materials Science & Engineering B **1021**, 1027 (2011).
[18] X. L. Li, X. Y. Zhu, T. L. Duan, and Y. T. Qian, Solid State Communications **526**, 529 (2006).
[19] Y. Liu, J. Zhan, J. Zeng, Y. Qian, K. Tang, W. Yu, Journal of Materials Science Letters **1865**, 1867 (2001) .
[20] F. Tavakoli, M. Salavati-Niasari, F. Mohandes, Materials Letters **133**, 136 (2013).
[21] F. Tavakoli, M. Salavati-Niasari, D. Ghanbari, K. Saberyan, S. M. Hosseinpour-Mashkani, Materials Research Bulletin **14**, 20 (2014).
[22] M. Ghanbari, M. Bazarganipour, M. Salavati-Niasari, Separation and Purification Technology **27**, 36 (2017) .
[23] M. R. Johan, K. Si-wen, N. Hawari, N. Azri, K. Aznan, International Journal of Electrochemical Science **4942**, 4950 (2012).
[24] M. Chen, Y. Zhao, S. Yu, Food Chemistry **543**, 550 (2014).
[25] H. E. Khoo, A. Azlan, S. T. Tang, S. M. Lim, Food & Nutrition Research **1**, 21 (2017).
[26] B. Sharma, M. K. Rabinal, Journal of Alloys and Compounds **198**, 202 (2013).